Session I - 1.5

SOLAR CYCLE EVOLUTION OF PROMINENCES AND ERUPTIONS

https://doi.org/10.1017/S1743921313010910 Published online by Cambridge University Press

Nature of Prominences and their role in Space Weather
Proceedings IAU Symposium No. 300, 2013
B. Schmieder, J. Malherbe & S. T. Wu, eds.

doi:10.1017/S1743921313010910

Unusual migration of the prominence activities in recent solar cycles

Masumi Shimojo

National Astronomical Observatory of Japan
2-21-1, Osawa, Mitaka, Tokyo, 181-8588, Japan
email: masumi.shimojo@nao.ac.jp

Abstract. We investigated the prominence eruptions and disappearances observed with the Nobeyama Radioheliograph during over 20 years for studying the anomaly of the recent solar cycle. Although the sunspot number of Cycle 24 is smaller than the previous one dramatically, the occurrence rate, size and radial velocity of the prominence activities are not changed significantly. We also found that the occurrence of the prominence activities in the northern hemisphere is normal from the duration of the cycle and the migration of the producing region of the prominence activities. On the other hand, the migration in the southern hemisphere significantly differs from that in the northern hemisphere and the previous cycles. Our results suggest that the anomalies of the global magnetic field distribution started at the solar maximum of Cycle 23.

Keywords. Prominence, solar cycle, microwave

1. Introduction

The solar activity of the recent solar cycles 23–24, shows significant differences from the previous cycles that were observed over the course of half of a century with modern instruments such as a magnetograph. The noticeable differences are the long cycle duration of Cycle 23 and the low activity of Cycle 24. Many authors have already reported other differences (Livingston *et al.* 2012, Petrie 2012, Wang *et al.* 2009, Gopalswamy *et al.* 2012, Shiota *et al.* 2012, Svalgaard & Kamide 2013, Lee *et al.* 2009, Wang *et al.* 2009, Thompson *et al.* 2011). To understand the anomalies of the solar activity in the recent solar cycles, we need to investigate the global distribution and evolution of the photospheric magnetic field. One way is to investigate directly the magnetic field distribution using the magnetograms. However, it is relatively difficult to understand an outline of the global magnetic field distribution because the magnetograms include the numerous fine structures. Dark filaments were used for understanding the global magnetic field distribution because they always lie on a magnetic neutral line. The Solar-Geophysical Data (SGD) published by NOAA National Geophysical Data Center had carried the Carrington maps that indicate the locations of dark filaments until the 1990s for this purpose.

The Nobeyama Radioheliograph (NoRH) is an interferometer in the microwave range, and can observe the thermal emission from a prominence well. Long-term studies were performed using this detection technique to understand polarity reversal (Copalswarmy *et al.* 2013a) and the relation between prominence activity and coronal mass ejections (Copalswarmy *et al.* 2013b) Based on the advantage of the NoRH for prominence observations, Shimojo *et al.* (2006) developed a semi-automatic detection method of prominence eruptions and disappearances for the NoRH data, and made a butterfly diagram of the prominence eruptions and disappearances. Considering that all dark filaments disappear

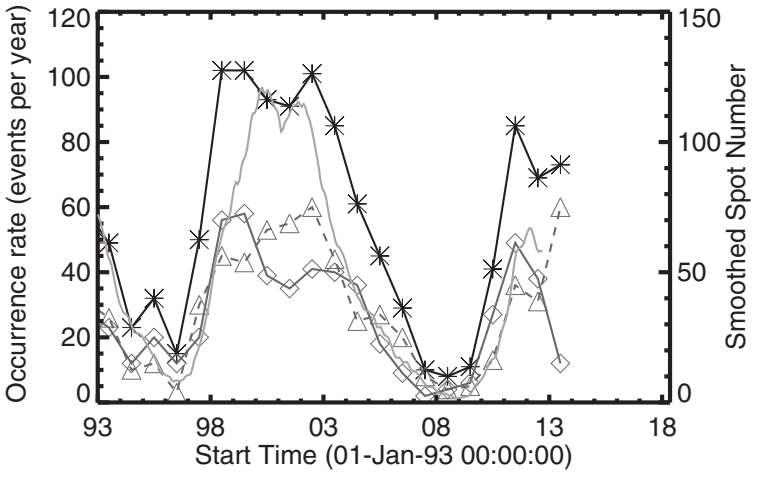

Figure 1. The occurrence rate of the prominence activities and sunspots from 1993 to 2013. The dark-gray line & diamond and the dark-gray dashed line & triangles show the occurrence rate in the northern and southern hemisphere. The black line is the total. The light gray line indicates the smoothed sunspot number.

by erupting and/or falling down, the distribution of the prominence eruptions and disappearances indicate that of the dark filaments. For this reason, the prominence eruption and disappearance are not distinguished and they are called "prominence activity" in this paper. To understand the global distribution and evolution of magnetic field of the Sun, we applied the prominence activity detection method developed by Shimojo *et al.* (2006) to over 20 years of NoRH data (July 1992 – March 2013) and detected 1131 events. Based on the events, we made the prominence activity database that includes the time, size, position, radial velocity and MPEG movie of them. The database is available at the website of the Nobeyama Solar Radio Observatory of the National Astronomical Observatory of Japan (http://solar.nro.nao.ac.jp/norh/html/prom_html_db/ see. Shimojo 2013).

From the next section, we show the solar cycle dependence of the occurrence rate, size, radial velocity of the prominence activities, and describe the migration of the producing region.

2. Solar cycle dependence of the occurrence, size & radial velocity

2.1. *Occurrence rate of prominence activities*

Figure 1 shows the time variations of the occurrence rate of the prominence activities and sunspots from 1993 to 2013. The value of 2013 hasa large uncertainty because the database includes only three months' data. The sunspot number in the figure is the six-month running mean calculated from the data that are released by the Solar Influence Data Center of the Royal Observatory of Belgium (SIDC-team 1992–2013).

Basically, the number variation of the the prominence activities is similar to that of the sunspot, but there are significant differences in the peak time of the values. The first peak of the prominence activities is faster than that of the sunspot number. It maybe caused by the high-latitude prominence activities that has no connection to sunspots as discuss in Copalswarmy *et al.* 2013a. The second peak of the prominence is delayed from the second peak of the sunspot number. We do not know what does caused the difference of the second peak. Although the sunspot number of Cycle 24 is smaller than that of

https://doi.org/10.1017/S1743921313010910 Published online by Cambridge University Press

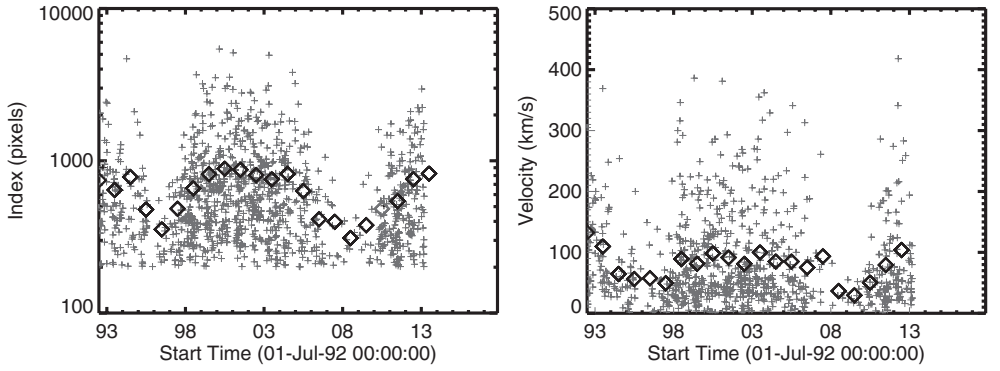

Figure 2. The time variation of the size (left panel) and the radial velocity (right panel).

the previous one significantly (about 50% down), the occurrence rate of the prominence activities is decreased only by 10%.

When we pay attention to the timing of the minimum values between Cycles 22 and 23, the figure shows that the number of the prominence activities (in the northern/southern hemisphere) and the sunspots became the minimum in 1996. On the other hand, between Cycles 23 and 24, the timings of the minimum values are different. Although the number of prominence activities occurring in the northern hemisphere became the minimum in 2007, the data of the sunspots and the prominence activities in the southern hemisphere indicates that the minimum year is 2008. The number of prominence activities suggests that the solar cycle period of the southern hemisphere in Cycle 23 is longer than the period of the northern hemisphere, 11 years.

2.2. *Size and radial velocity of prominence activities*

In this study, to evaluate of the size of the prominence, the number of the pixels that are brighter than 6 times of the average brightness temperature of the day at the pixel is used. We name the number of the bright pixels "Index". Since the pixel size of NoRH is 2.5 arcsec, the Index "1000" is correspond with about 6×10^4 km.

The left panel of Figure 2 shows the solar cycle dependence of the size. The small gray plus indicates the size of each prominence activity and the big diamonds indicate the yearly averages. Based on the yearly averages, the size of the prominence activities is only decreased around the solar minimum. However it is not correct understanding because the size distributions of prominence activities shows the power-law distribution (Shimojo *et al.* 2006). Figure 3 shows the size distribution of each phase of the solar cycles. Except the solar minimum, the distributions of the phases show the power-law and the index is 2.5∼2.9. Considering the precision of the fitting, we conclude that there is no difference between the values. In the solar minimum, the prominence activities that are larger than 1000 Index do not happen.

The right panel of Figure 2 shows the solar cycle dependence of the radial velocity. The radial velocity of the prominence activities is derived from the center of gravity of the brightness temperature. Hence, the radial velocities of our database are slower than the other results (Copalswarmy *et al.* 2013b). Only the events that have the upward velocities are plotted in the figure, because there are the events that have only the downward velocities (for example, the observation was started at the decay phase of the eruption). The small gray plus symbol in the figure indicates the radial velocity of each prominence activity and the big diamonds indicate the yearly averages. The figure of

https://doi.org/10.1017/S1743921313010910 Published online by Cambridge University Press

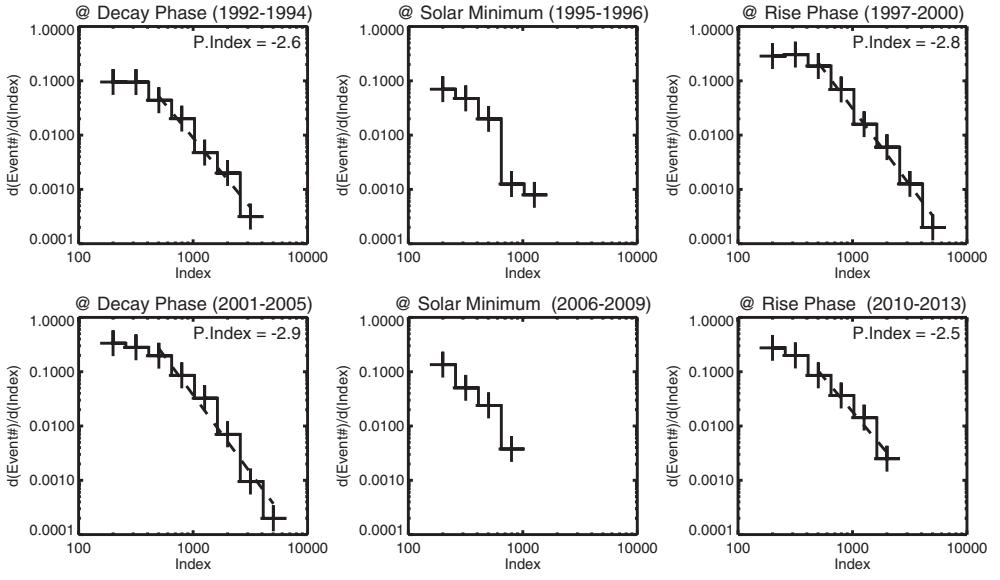

Figure 3. The size distribution of each phase.

the radial velocity is similar to that of the size, the yearly average of the radial velocity is about 100 km/s except the solar minimum. The difference might be caused by the producing region of the prominence activities. Except the solar minimum , most of the prominence activities occurred near the active regions, or the quiet regions with relative strong magnetic field that is caused by "the rush to the pole" magnetic field motion. Hence, the magnetic field strength around the prominence activities is larger than that in the solar minimum and the upward velocity becomes high.

3. Migration of the producing region of the prominence activities

3.1. *Northern hemisphere*

Figure 4 is the butterfly diagram of the prominence activities, and covers over the 20 years that correspond to the period from the decay phase of Cycle 22 to the rising phase of Cycle 24. We concentrate on the northern hemisphere at this subsection. The production region of the prominence activities is expanding toward the pole in the rising phase of the solar cycle. When the polemost prominence activity occurs near the pole around the solar maximum, the polarity reversal has taken place. The appearance region of dark filaments observed in H-alpha line also shows the similar poleward expansion and the relation with the polarity reversal (Waldmeier 1973, Topka *et al.* 1982, Mouradiam & Soru-Escaut 1994, Makarov *et al.* 2001, Li *et al.* 2009), and Gopalswamy *et al.* (2003b) also reported the relation between the prominence activities and the polarity reversal. We derive the expansion velocity from the polemost prominence activities in the butterfly diagram. The expansion velocities in the northern hemisphere are 5.9 m/sec at Cycle 23 and 5.2 m/sec at Cycle 24. Hathaway & Rightmire (2010) derived the latitudinal profile of the meridional flow speed from the magnetic features observed by the Michelson Doppler Imager (MDI) aboard the Solar and Heliospheric Observatory (SOHO) from May 1996 to June 2009. The expansion velocity that is derived from the prominence activities corresponds to the meridional flow speed around 60 degrees latitude. The coincidence suggests that the poleward migration of the polemost prominence activities

https://doi.org/10.1017/S1743921313010910 Published online by Cambridge University Press

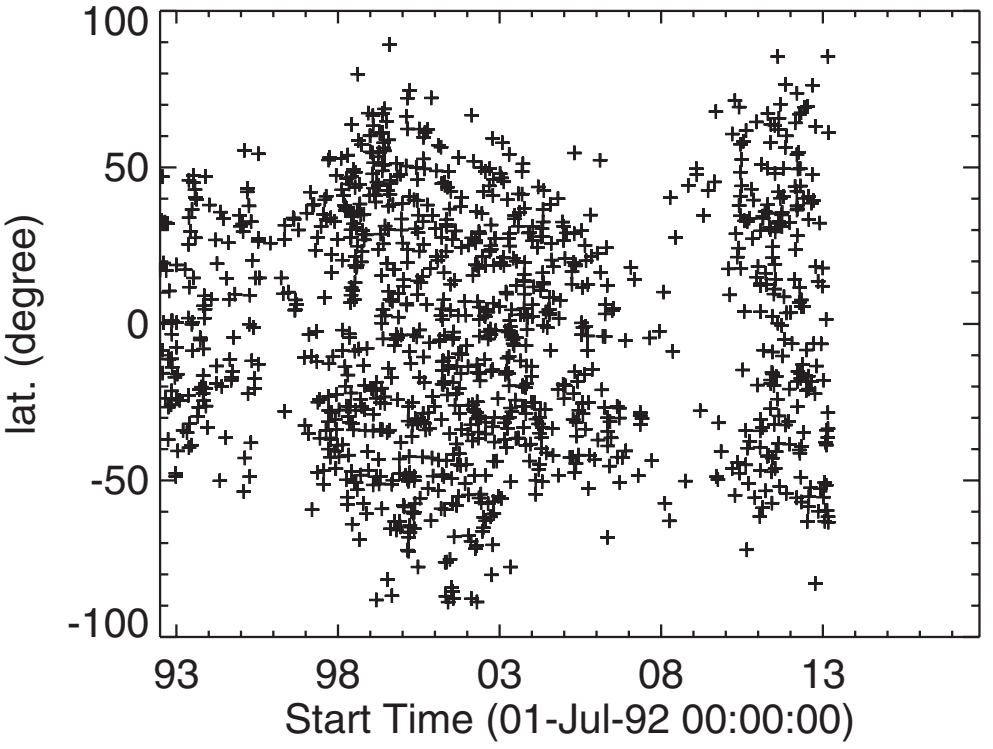

Figure 4. The butterfly diagram of the prominence activities.

is an indicator of the meridional flow. Our result is slower than the expansion velocity ($\sim$ 10 m/sec) derived from the dark filaments observed in Cycle 19 (Topka *et al.* 1982). The disagreement might show that the meridional flow speed in Cycle 23–24 is slower than that in the previous cycles.

After the solar maximum, the latitude of the prominence activity region is shrinking toward to the equator. The variation of the source latitude agrees with the variation of the active region filaments rather than all dark filaments (Mouradiam & Soru-Escaut 1994). This suggests that most of the prominence activities in the decay phase of a solar cycle are produced by the prominences in active regions. Li (2010) investigated the appearance region of the dark filaments in Cycle 16–21, and suggests that a third-order polynomial curve could give a satisfactory fit to the monthly mean latitude of dark filaments. We applied the fitting to our database, and found that the mean latitude in the northern hemisphere at Cycle 23 is similar to that at the previous cycles given in Figure 4 of Li (2010).

According to the observing facts, we can say that the migration of the source region of the prominence activities in the northern hemisphere at Cycle 23–24 is similar to the previous cycles. When the butterfly diagram of prominence activities that is shifted 11 years is overlaid on Figure 4 in the northern hemisphere (the overlaid figure is not included in the paper), the prominence activities that occurred after the solar maximum of Cycle 23 trace the butterfly diagram of the prominence activities from the decay phase of Cycle 22 to the rising phase of Cycle 23. The fact also suggests that the northern hemisphere at Cycle 23–24 is normal from the point of view of prominence activities.

https://doi.org/10.1017/S1743921313010910 Published online by Cambridge University Press

3.2. *Southern hemisphere*

At the rising phase of Cycle 23, the producing region of the prominence activities is expanding toward the pole in the southern hemisphere. The expansion velocity is 7.3 m/sec and is faster than that in the northern hemisphere. The same trend of the hemispheric asymmetry is reported by Hathaway & Rightmire (2010), and it also suggests that the poleward migration of polemost prominence activities indicates the meridional flow.

After the solar maximum of Cycle 23, the migration of the source region of the prominence activities became unusual. Although the difference of the mean latitude migration in the northern and southern hemisphere at the previous cycles is small (Li 2010), the migration of the southern hemisphere is significantly different from that of the northern hemisphere at Cycle 23 and the previous cycles. The monthly mean latitude in the southern hemisphere did not decrease quickly after the solar maximum as in the northern hemisphere, and it stayed over −30 degree latitude after 2006. Figure 4 shows that the prominence activities occurred at over −50 degree latitude after 2006. Surprisingly, some prominence activities occurred at over −60 degrees latitude even in 2008, the solar minimum year. So, such high latitude prominence activities caused the unusual migration in the decay phase at the southern hemisphere.

The rising phase of Cycle 24 began in 2009. Although we can see the prominence activities associated with the active regions from late 2009, the expansion of the source region in the southern hemisphere is not seen in the butterfly diagram of prominence activities. Only the two prominence activities occurred at over −65 degrees latitude after 2009.

4. Summary

In the previous sections, we showed that the occurrence of the prominence activities in the northern hemisphere is normal from the duration of the cycle and the migration of the producing region of the prominence activities. On the other hand, the migration in the southern hemisphere significantly differs from that in the northern hemisphere and the previous cycles. The unusual migration in the southern hemisphere started from the solar maximum of Cycle 23. It is clear that the unusual migration was caused by the anomalous prominence activities in the high-latitude region (over −50 degrees). However, the origin of the anomalies is hidden under the photoshere, and we need the progress of solar dynamo studies to fully understand the anomalies. A polemost prominence activity is a good indicator of the meridional flow. The tracing of the polemost filament or prominence in the previous cycles might be one of the keys to understand the meridional flow and the solar activities.

References

Gopalswamy, N., Lara, A., Yashiro, S., & Howard, R. A. 2003 *ApJ*, 598, L63

Gopalswamy, N., Shimojo, M., Lu, W., Yashiro, S., Shibasaki, K., & Howard, R. A. 2003 *ApJ*, 586, 562

Gopalswamy, N., Yashiro, S., Mäkelä, P., Michalek, G., Shibasaki, K., & Hathaway, D. H. 2012 *ApJ*(Letter), 750, L42

Hathaway, D. H. & Rightmire, L. 2010 *Science*, 327, 1350

Lee, C. O., Luhmann, J. G., Zhao, X. P., Liu, Y., Riley, P., Arge, C. N., Russell, C. T., & de Pater, I. 2009 *Solar Phys.*, 256, 345

Li, K. J., Li, Q. X., Gao, P. X., & Shi, X. J. 2008 *JGR*, 113, A11108

Li, K. J., 2010, *MNRAS*, 405, 1040

Livingston, W., Penn, M. J., & Svalgaard, L. 2012 *ApJ*(Letter), 757, L8

https://doi.org/10.1017/S1743921313010910 Published online by Cambridge University Press

Makarov, V. I., Tlatov, A. G., & Sivaraman, K. R. 2001 *Solar Phys.*, 202, 11
Mouradiam, I. Z. & Soru-Escaut, I. 1994 *A&A*, 290, 279
Nakajima, H., *et al.* 1994 *Proceeding of the IEEE*, 82, 5, 705
Petrie, G. J. D. 2012 *Solar Phys.* 281, 577
Shimojo, M.,Yokoyama, T., Asai, A., Nakajima, H., & Shibasaki, K. 2006 *PASJ*, 58, 1, 85
Shimojo, M., 2013 *PASJ*, 65, S1, in press
Shiota, D., Tsuneta, S., Shimojo, M., Sako, N., Orozco Suárez, D., & Ishikawa, R. 2012 *ApJ*, 753, 157
SIDC-team 1992–2013 World Data Center for the Sunspot Index, Royal Observatory of Belgium, Monthly Report on the International Sunspot Number, online catalogue of the sunspot index: http://sidc.oma.be/sunspot-data/
Svalgaard, L. & Kamide, Y., 2013, *ApJ*, 763, 23
Thompson, B. J., *et al.* 2011 *Solar Phys.*, 274, 29
Topka, K., Moore, R., Labonte, B. J., & Howard, R. 1982 *Solar Phys.*, 79, 231
Waldmeier, M. 1973 *Solar Phys*, 28, 389
Wang, Y.-M., Robbrecht, E., & Sheeley, N. R. Jr. 2009 *ApJ*, 707, 1372